

# Ductility demands and reduction factors for 3D steel structures with pinned and semi-rigid connections

Mario D. Llanes-Tizoc<sup>1a</sup>, Alfredo Reyes-Salazar<sup>\*1</sup>, Sonia E. Ruiz<sup>2b</sup>, Eden Bojorquez<sup>1c</sup>,  
Juan Bojorquez<sup>1d</sup> and Jesus M. Leal Graciano<sup>1e</sup>

<sup>1</sup>Facultad de Ingeniería, Universidad Autónoma de Sinaloa, Culiacán, Sinaloa, 80040, México

<sup>2</sup>Instituto de Ingeniería, Universidad Nacional Autónoma de México, Ciudad Universitaria, Coyoacán, Ciudad de México, México

(Received September 27, 2018, Revised March 9, 2019, Accepted March 17, 2019)

**Abstract.** A numerical investigation regarding local ( $\mu_L$ ) and story ( $\mu_S$ ) ductility demand evaluation of steel buildings with perimeter moment resisting frames (PMRF) and interior gravity frames (IGF), is conducted in this study. The interior connections are modeled, firstly as perfectly pinned (PP), and then as semi-rigid (SR). Three models used in the SAC steel project, representing steel buildings of low-, mid-, and high-rise, are considered. The story ductility reduction factor ( $R_{\mu S}$ ) as well as the ratio ( $Q_{GL}$ ) of  $R_{\mu S}$  to  $\mu_L$  are calculated.  $\mu_L$  and  $\mu_S$ , and consequently structural damage, at the PMRF are significant reduced when the usually neglected effect of SR connections is considered; average reductions larger than 40% are observed implying that the behavior of the models with SR connections is superior and that the ductility detailing of the PMRF doesn't need to be so stringent when SR connections are considered.  $R_{\mu S}$  is approximately constant through height for low-rise buildings, but for the others it tends to increase with the story number contradicting the same proportion reduction assumed in the Equivalent Static Lateral Method (ESLM). It is implicitly assumed in IBC Code that the overall ductility reduction factor for ductile moment resisting frames is about 4; the results of this study show that this value is non-conservative for low-rise buildings but conservative for mid- and high-rise buildings implying that the ESLM fails evaluating the inelastic interstory demands. If local ductility capacity is stated as the basis for design, a value of 0.4 for  $Q_{GL}$  seems to be reasonable for low- and medium-rise buildings.

**Keywords:** steel building; moment resisting frames; local and story ductility; ductility and force reduction factors; pinned and semi-rigid connections; 3D models; nonlinear analysis

## 1. Introduction

Several alternatives for structural systems are used in structures to support the force demands produced by different types of loading. In the case of seismic loading, the induced forces caused by the action of moderate and severe earthquakes will significantly depend on the structural energy dissipation capacity. This issue is particularly important for steel structures since dissipation of energy is expected to occur for several sources, which mostly characterizes the ductility capacity ( $\mu$ ). Many mechanisms contribute to the energy dissipation in actual

steel building structures. In the case of seismic analysis of steel buildings, this dissipation is approximately considered in two ways: an equivalent viscous damper is used to model the energy dissipation at deformations within the elastic limit while the dissipated energy due to yielding of the material is considered by including the inelastic relationship between resisting forces and deformations. However, as additionally pointed out below, some sources of energy dissipation are not considered as that produced by the flexibility of shear connections.

Thus the  $\mu$  parameter is a critical factor which importantly defines the inelastic structural behavior and can offer an appropriate design parameter (Osteraas and Krawinkler 1990). The dissipation of energy due to yielding of the material (inelastic behavior) is considered through the ductility reduction factor ( $R_\mu$ ). In this regard, the different levels of ductility, namely local ( $\mu_L$ ), story ( $\mu_S$ ) and global ( $\mu_G$ ), existing in a building must be considered (Newmark and Hall 1982). Because there is a significant number of experimental studies about ductility of individual members (beams and columns) some researchers (Newmark and Hall 1982, Osteraas and Krawinkler 1990) suggest using local ductility ( $\mu_L$ ) as the basis for design. Consequently, it is important to establish a relationship between the ductility reduction factor at a global level ( $R_{\mu S}$ ) and the local ductility capacity ( $\mu_L$ ) (Uang and Bruneau 2018).

The  $R_\mu$  parameter and the overstrength factor ( $R_\Omega$ )

---

\*Corresponding author, Professor

E-mail: reyes@uas.edu.mx

<sup>a</sup>Ph.D. Student

E-mail: llaneg32@gmail.com

<sup>b</sup>Professor

E-mail: sruizg@iingen.unam.mx

<sup>c</sup>Professor

E-mail: eden\_bmseg@hotmail.com

<sup>d</sup>Research Fellow

E-mail: jbm\_squall\_cloud@hotmail.com

<sup>e</sup>Research Fellow

E-mail: martin\_leal2@hotmail.com

constitute the main components of the modification factor  $R$  (also known as force, or strength, reduction factor) used in seismic codes (Uang 1991a, Uang 1991b, Miranda and Bertero 1994, Witthaker *et al.*, 1999, Uang and Bruneau 2018). These factors allow to design structures for forces much smaller than those obtained by elastic analyses. It is worth to mention, however, that the magnitude of this factor represents one of the most controversial aspects related to the seismic design previsions.

For the case of steel buildings, moment resisting frames (MRF) are commonly used as the structural system for lateral resistance because they provide maximum flexibility for space utilization. The basic structural system, however, has been modified over the years particularly in developed countries like USA; during the last three decades, because of the minor axis bending fragility and the expensive of fully restrained (FR) connections, MRF are used on two frame lines in each direction, usually at the perimeter. It results in a system with perimeter moment resistant frames (PMRF) and interior gravity frames (IGF) with perfectly pinned (PP) connections, which are designed to support the total seismic lateral loads and the total gravity loads, respectively.

One of the main assumptions regarding the idealization of this structural system is to neglect the contribution of the interior connections. These assumptions can be accepted for practical reasons but it is necessary to recognize that the FR and PP connections have a certain grade of flexibility and stiffness, respectively; in other words, all connections are essentially semi-rigid (SR) with different degrees of flexibility. The implication of this is that considering the contribution of the stiffness and dissipation of energy at connections could have a substantial effect on the structural response in terms of ductility demands. Modeling connection as FR or PP is nothing but an assumption to simplify calculations but it is a disadvantage in current analytical procedures. These and other simplifications can result in erroneous values in the response estimation, namely interstory drifts and resultant stresses.

As it will be additionally explained below, the central objective of this research is to compare the ductility demands and the associated ductility reduction factor of steel building structures with PMRF and IGF with PP connections, with those of the same buildings by modeling the interior connections in a more realistic way, i.e., as SR, where the effect of the stiffness and dissipated energy at the interior connections is explicitly considered.

## 2. Literature review

Many investigations have been conducted regarding the evaluation of the  $\mu$ ,  $R_\mu$  and  $R$  factors for steel and concrete buildings modeled as single of degree of freedom (SDOF) systems. The  $R$  parameter was firstly introduced in ATC-3-06 (1978) in the late 70s with the aim of reducing the elastic base shear. Among the first investigations it can also be mentioned that by Newmark and Hall (1982) where a procedure to relate  $R_\mu$  and  $\mu$  was proposed. Hadjian (1989) studied the reduction of the spectral accelerations to

account for the inelastic behavior of structures. Significant contributions were also derived from many other studies (Miranda and Bertero 1994, Ordaz and Perez-Rocha 1998, Borzi and Elnashai 2000, Arroyo-Espinoza and Terán-Gilmore 2003, Levy *et al.* 2006, Karmakar and Gupta 2006, Ayoub and Chenouda 2009, Rupakhety and Sigbjörnsson 2009).

The magnitude of the  $\mu$ ,  $R_\mu$  and  $R$  factors for multi degree of freedom (MDOF) systems has also been investigated. Nassar and Krawinkler (1991) studied the relationship between force reduction factors and ductility for simplified MDOF systems. Santa-Ana and Miranda (2000) studied the strength reduction factors for several steel frames modeled as plane MDOF systems. Elnashai and Mwafy (2002) investigated the relationship among the lateral capacity, the design force reduction factor, the ductility factor and the overstrength factor for reinforced-concrete buildings. Reyes-Salazar (2002) studied the ductility capacity of plane steel moment-resisting frames; local, story and global ductility were considered. Karavasilis *et al.* (2008) proposed simplified expressions to estimate the behavior factor of plane steel moment resisting frames. Chopra (2008) studied the force reduction factors for MDOF systems modeled as shear buildings. Cai *et al.* (2009) estimated ductility reduction factors for MDOF systems by modifying ductility reduction factors of SDOF. Mohsenian and Mortezaei (2018) evaluated the response reduction factors of braced frames using vertical links as passive energy dissipaters. Significant contributions can also be found in other studies (Whittaker 1999, Ganjavi and Hao 2012, Abdollahzadeh and Banihashemi 2013, Abdollahzadeh and Faghihmaleki 2014, Reyes-Salazar *et al.* 2015, Serror *et al.* 2014, Hetao *et al.* 2016, Abdi *et al.* 2015).

The seismic behavior of steel buildings considering connections as SR has been studied by many researchers, some of the studies were based on simple models resembling SDOF systems and some others were based on simplified MDOF systems. Nader and Astaneh (1991) and Leon and Shin (1995) showed that the seismic response of steel frame with SR connections can be smaller than that of frames with FR connections; one of the reasons for this is that SR connections introduce an important source of energy dissipation. Kishi *et al.* (1993) proposed design aids to determine the values of the connection parameters with the help of a set of monograms, which allow the engineer to quickly determine the moment-rotation curve for a given connection. Elnashai *et al.* (1998) presented the results of experiments on the seismic behavior of SR steel frames with top, bottom and web angles; they demonstrated that the type of bolted connection used in this study exhibits sufficient ductility and stable hysteretic behavior. Reyes-Salazar and Haldar (2000) demonstrated that the maximum values of basal shears and interstory displacements of steel plane frames under the action of ground movements caused by earthquakes were reduced when SR connections were used. In another study, Reyes-Salazar *et al.* (2009) demonstrated that neglecting the capacity of IGF to resist lateral loads, or ignoring the rigidity of PP connections, results in conservative structural design. Liu (2010)

provides a discussion of the mathematic modeling of connections for designing structures subject to monotonic or cyclic loading; a review of the Ramberg-Osgood, Richard-Abbott, and Menegotto-Pinto models is performed. Reyes Salazar *et al.* (2012) showed that modeling buildings as two-dimensional structures results in interstory shears and maximum drifts (MD) larger than those of three-dimensional structures and that the differences are much larger when SR connections are considered in the IGF of the three-dimensional models. Hadianfard (2012) proposed a method to reduce the computational works in the seismic response of steel frames with SR connections. Liu and Lu (2014) proposed a method to analyze the dynamic response behavior of suspended building structures with SR connections. More recently Reyes-Salazar *et al.* (2016) estimated the non-linear seismic response of steel buildings with MRMs at the exterior and IGF in the interior considering the interior connections as SR; what they concluded was that the effect of the energy dissipated at the SR connections should not be neglected and that the reduction in resultant stresses when considering the SR connections (even if the rigidity is small) could be significant. Bayat and Zahrai (2017) evaluated the seismic performance of hybrid steel frames defined as mixture of rigid and semi-rigid connections.

Hadianfard and Razani (2003) estimated the failure probability of steel frames considering SR connections using the Monte Carlo simulation technique. Kartal (2010) developed a finite element program in Fortran Language for the numerical analysis of SR connections in terms of the rigidity which were modeled as rotational springs. Gholipour *et al.* (2015) evaluated seismic performance of dual steel moment-resisting frames with mixed use of rigid and semi-rigid connections. Shoostari *et al.* (2015) evaluated the nonlinear static response applied to semi-rigid steel glabed frames.

The above mentioned studies represent a significant advancement regarding the state of the art of the  $\mu$ ,  $R_\mu$  and  $R$  parameters, particularly for steel building structures. However, most of them were for SDOF systems, therefore the inelastic behavior and energy dissipation of structural elements existing in actual buildings were not explicitly considered. Reyes-Salazar and Haldar (1999, 2000, 2001a, 2001b, 2002) showed that the dissipated energy of steel frames with welded (FR) or SR connections has an important effect on the response and that the values of ductility demands and strength reduction factors depend on the plastic mechanism formed in the frames as well as on the loading, unloading and reloading process at plastic hinges or in the SR connections; it is worth to mention that it is not possible to observe plastic mechanisms on SDOF systems. For the case of previous studies considering MDOF systems, plane shear buildings, plane moment resisting steel frames or a limited level of inelastic deformation were considered; modeling buildings as plane frames may not represent their actual behavior since the participation of some elements is not considered and the contribution of some vibration modes are ignored. In addition, a limited level of inelastic deformation is not associated to the ductility capacity and consequently to the

maximum force reduction factors. Moreover, the effect of the stiffness and dissipated energy at the interior connections on the  $\mu$  and  $R_\mu$  parameters of steel buildings with PMRF and IGF, as well as a relationship between the  $R_\mu$  factor and the local ductility factor have not been studied.

### 3. Objectives

The general objective of this research is to calculate the nonlinear seismic responses of steel buildings with PMRF and IGF modeled as complex-3D-MDOF systems, considering the interior connections firstly as PP and then as SR in such a way that the effect of the stiffness and dissipated energy at the interior connections is considered, with the aim of estimating the ductility demands and the associated ductility reduction factors for both types of connections. Several levels of structural deformation are considered; the last one will correspond to the structural capacity and consequently to the ductility capacity. The specific objectives are:

- (1) Calculate the local ductility demands for individual structural elements (beams) in terms of curvatures as well as story ductility demands for the building models with PP connections and compare them with those of the same buildings with interior SR connections.
- (2) Calculate the magnitude of ductility reduction factors.
- (3) Estimate a ratio of ductility reduction factor to local ductility.

### 4. Procedure, methodology and structural models

#### 4.1 Parameters of the study

Three three-dimensional (3D) building models, representing steel building structures of low-, mid- and high-rise, and fifteen strong seismic motions, are considered in the study. The connections of the IGF are modeled, firstly as PP, and then as SR. The behavior of the SR connections is nonlinear even for small levels of deformation, their relative rigidity is calculated according to the Beam Line Theory (Disque 1964) and the Richard Model (Richard and Abbot 1975, Richard 1993). This theory is included in the PRCONN program (Richard, 1993), which is used in this study to determine the connection rigidities. Local and story ductility demands as well as ductility reduction factors are calculated. The used seismic motions are scaled up to get several levels of structural demands, including small (elastic behavior), moderate and significant (close to the collapse) deformations. The Ruaumoko computer program (Carr 2011) is used to perform the required step by step nonlinear seismic analyses. The Newmark Constant Average Acceleration Method is used to numerically evaluate the seismic response. The lumped mass matrix, Rayleigh Damping and large displacement effects are also considered. No strength degradation member, bilinear behavior with 5% of post-yielding stiffness as well as

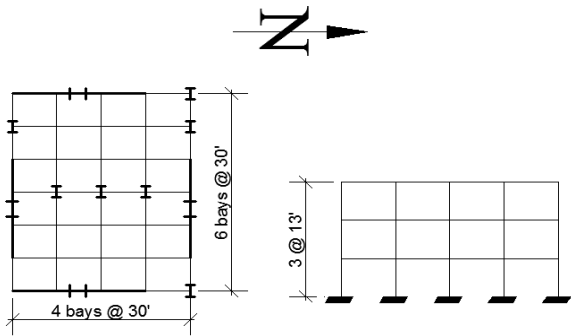


Fig. 1 Plan and elevation, 3-Level Model

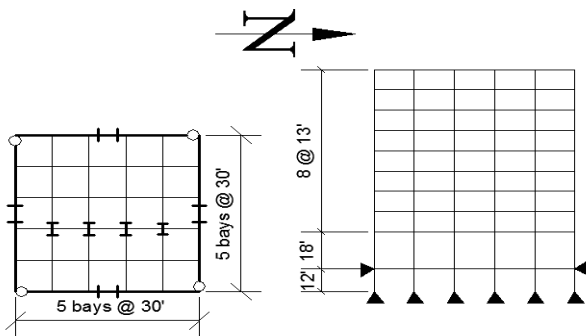


Fig. 2 Plan and elevation, 9-Level Model

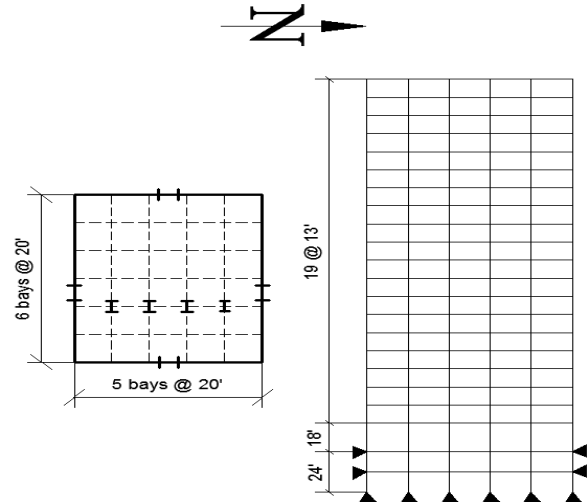


Fig. 3 Plan and elevation, 20-Level Model

concentrated plasticity are assumed in the analyses. To define member plasticization, the axial load-bending moment interaction given by the yield interaction surface proposed by Chen and Atsuta (1971) is considered.

#### 4.2 Structural models with interior PP connections

Three steel building models that were particularly designed by three consulting firms to be used in the SAC Steel Project (FEMA 355C, 2000), to study the seismic behavior of low-, mid-, and high-rise buildings, are considered in this paper for numerical evaluations of the issues discussed earlier. They are the Pre-Norhridge steel building structure models with 3-, 9- and 20-levels located in Los Angeles Area. For the case of PP connections, they will be denoted hereafter as Models PP1, PP2, and PP3 for the 3-, 9- and 20-level buildings, respectively. It is considered that these buildings meet all the existing requirements at the time of the development of the SAC Project according to the codes of Los Angeles (UBC 1997). The fundamental periods of these models associated to the first mode of lateral vibration are 1.03s, 2.38s and 4.07s and their geometry can be seen (plan and elevation) in Figs. 1, 2 and 3, respectively. The PMRM are represented by thicker lines. As it can be seen, the buildings are essentially symmetrical in plan, so significant torsional moments are not expected to occur. The columns of the PMRF of the 3-level model are fixed at the base while those of the 9- and 20-level models are pinned. For the three models, the columns of the IGF are considered to be pinned at the base. The 9-level building has a basement and the 20-level building has two. The yield strength of the beams is 36 ksi and that of the columns is 50 ksi. It must be noted that

for the case of the 3-level model there is no intersection of the PMRM so there is no bending moment with respect to the weak axis. For the case of the 9-level model, the perimeter frames intersect in the corner; in this case, however, beam-column connections are built as pinned to eliminate bending relative to the weak axis. In the 20-level model, the corner columns are made of steel box sections to eliminate the minor axes bending problem. All structural elements of the PMRF are assumed to be connected by fully restrained connections and are modeled as beam-column elements whose nonlinear behavior is as defined above in Section 4.1. Damping is considered to be 3% of the critical. Buildings are modeled as complex MDOF systems. Each column and each girder are represented by a structural element. The slab is modeled as a rigid floor diaphragm as considered in a FEMA Report (FEMA 2000). Each node has six degrees of freedom. The total number of degrees of freedom is 846, 3408, 8574, for Models PP1, PP2 and PP3, respectively. Section sizes of the SAC Models are given in Tables 1-2. Additional information about the models can be obtained from the above mentioned FEMA Report.

#### 4.3 Structural models with interior SR connections

It was stated above that the connections of the IGF are, firstly modeled as PP, and then more realistically, as SR. It is worth to mention that even though in seismic codes it is not generally accepted the seismic design of relatively tall buildings like the 20-level model according the equivalent static procedures, it would be of interest to study some aspects of the seismic behavior of this building considering the interior connections as SR. Double web angles (DWA) were used at the interior connections. The SR connections were represented by nonlinear rotational springs, placed at the ends of the beams belonging to the gravity frames. Thus an additional node is needed for each connection. The models with SR connections are denoted hereafter as SR1, SR2 and SR3, for the 3-, 9- and 20-level buildings, respectively; the corresponding total number of degrees of freedom are 2496, 6696 and 17556. Table 3 contains the connection components. The fundamental periods

Table 1 Beam and column sections for the 3- and 9-level models

| Model   | Moment resisting frames (MRM) |          |          |         | Interior Gravity Frames (IGF) |         |        |
|---------|-------------------------------|----------|----------|---------|-------------------------------|---------|--------|
|         | Story                         | Columns  |          | Girder  | Columns                       |         | Beams  |
|         |                               | Exterior | Interior |         | Below Pent-House              | Others  |        |
| 3-Level | 1                             | W14×257  | W14×311  | W33×118 | W14×82                        | W14×68  | W18×35 |
|         | 2                             | W14×257  | W14×311  | W30×116 | W14×82                        | W14×68  | W18×35 |
|         | 3/Roof                        | W14×257  | W14×311  | W24×68  | W14×82                        | W14×68  | W16×26 |
| 9-Level | Basement-1                    | W14×370  | W14×500  | W36×160 | W14×211                       | W14×193 | W18×44 |
|         | 1                             | W14×370  | W14×500  | W36×160 | W14×211                       | W14×193 | W18×35 |
|         | 2                             | W14×370  | W14×500  | W36×160 | W14×211                       | W14×193 | W18×35 |
|         | 3                             | W14×370  | W14×455  | W36×135 | W14×159                       | W14×145 | W18×35 |
|         | 4                             | W14×370  | W14×455  | W36×135 | W14×159                       | W14×145 | W18×35 |
|         | 5                             | W14×283  | W14×370  | W36×135 | W14×120                       | W14×109 | W18×35 |
|         | 6                             | W14×283  | W14×370  | W36×135 | W14×120                       | W14×109 | W18×35 |
|         | 7                             | W14×257  | W14×283  | W30×99  | W14×90                        | W14×82  | W18×35 |
|         | 8                             | W14×257  | W14×283  | W27×84  | W14×90                        | W14×82  | W18×35 |
| 9/Roof  | W14×233                       | W14×257  | W24×68   | W14×61  | W14×48                        | W16×26  |        |

Table 2 Beam and column sections for the SAC 20-level model

| Story      | Moment resisting frames (MRM) |         |         | Interior Gravity Frames (IGF) |              |        |
|------------|-------------------------------|---------|---------|-------------------------------|--------------|--------|
|            | Columns                       | Girder  | Columns | Beams                         |              |        |
|            |                               |         |         | 40 feet span                  | 20 feet span |        |
| Basement-1 | 15×15×2.00                    | W24×335 | W14×22  | W14×550                       | W21×50       | W14×22 |
| Basement-2 | 15×15×2.00                    | W24×335 | W30×99  | W14×550                       | W24×68       | W16×26 |
| 1          | 15×15×2.00                    | W24×335 | W30×99  | W14×550                       | W21×50       | W14×22 |
| 2          | 15×15×2.00                    | W24×335 | W30×99  | W14×550                       | W21×50       | W14×22 |
| 3          | 15×15×1.25                    | W24×335 | W30×99  | W14×455                       | W21×50       | W14×22 |
| 4          | 15×15×1.25                    | W24×335 | W30×99  | W14×455                       | W21×50       | W14×22 |
| 5          | 15×15×1.25                    | W24×335 | W30×108 | W14×455                       | W21×50       | W14×22 |
| 6          | 15×15×1.00                    | W24×229 | W30×108 | W14×370                       | W21×50       | W14×22 |
| 7          | 15×15×1.00                    | W24×229 | W30×108 | W14×370                       | W21×50       | W14×22 |
| 8          | 15×15×1.00                    | W24×229 | W30×108 | W14×370                       | W21×50       | W14×22 |
| 9          | 15×15×1.00                    | W24×229 | W30×108 | W14×311                       | W21×50       | W14×22 |
| 10         | 15×15×1.00                    | W24×229 | W30×108 | W14×311                       | W21×50       | W14×22 |
| 11         | 15×15×1.00                    | W24×229 | W30×99  | W14×311                       | W21×50       | W14×22 |
| 12         | 15×15×1.00                    | W24×192 | W30×99  | W14×257                       | W21×50       | W14×22 |
| 13         | 15×15×1.00                    | W24×192 | W30×99  | W14×257                       | W21×50       | W14×22 |
| 14         | 15×15×1.00                    | W24×192 | W30×99  | W14×257                       | W21×50       | W14×22 |
| 15         | 15×15×0.75                    | W24×131 | W30×99  | W14×176                       | W21×50       | W14×22 |
| 16         | 15×15×0.75                    | W24×131 | W30×99  | W14×176                       | W21×50       | W14×22 |
| 17         | 15×15×0.75                    | W24×131 | W27×84  | W14×176                       | W21×50       | W14×22 |
| 18         | 15×15×0.75                    | W24×117 | W27×84  | W14×108                       | W21×50       | W14×22 |
| 19         | 15×15×0.75                    | W24×117 | W24×62  | W14×108                       | W21×50       | W14×22 |
| 20/Roof    | 15×15×0.50                    | W24×84  | W21×50  | W14×108                       | W21×44       | W12×16 |

Table 3 Elements of the SR connections

| MODEL    | Section | Web angle |        | Web screws |      |        |
|----------|---------|-----------|--------|------------|------|--------|
|          |         | Size (in) | Length | Number     | Gage | Φ (in) |
| 3-level  | W18×35  | 4×4×3/8   | 6      | 5          | 2.5  | 3/4    |
|          | W16×26  | 4×4×3/8   | 5.5    | 5          | 2.5  | 3/4    |
| 9-level  | W1×35   | 4×4×3/8   | 6      | 5          | 2.5  | 3/4    |
|          | W16×26  | 4×4×3/8   | 5.5    | 5          | 2.5  | 3/4    |
| 20-level | W14×22  | 4×4×1/4   | 5      | 4          | 2    | 3/4    |
|          | W12×16  | 4×4×3/8   | 4      | 3          | 2    | 3/4    |

associated to lateral vibration are 0.96s, 2.25s and 3.86s for the 3-, 9- and 20-level buildings, respectively.

#### 4.4 Seismic records

Fifteen strong motions, representative of the area where the structural models are located, are considered in the study. They are wide band strong motions, which were recorded at firm and intermediate soils; their predominant periods can be observed in Fig. 4. Their ground accelerations are larger than 0.3 g for a least 15 seconds. The horizontal components with the largest and smallest peak ground accelerations (PGA) are applied in the EW and NS structural directions, respectively; the other component is applied in the vertical direction. The data of the seismic records are shown in Table 4; they were obtained from the Data Set of the National Strong Motion Program (NSMP) of the United States Geological Sources (USGS). The individual pseudo-acceleration response spectra for 3% of

Table 4 Seismic records

| Designation | Record Information  | Magnitude<br>Mw | PGA |     | Period |     |
|-------------|---------------------|-----------------|-----|-----|--------|-----|
|             |                     |                 | NS  | EO  | NS     | EO  |
| LA1         | Imperial Valley,    | 6.9             | 178 | 261 | 0.5    | 0.4 |
| LA2         | Imperial Valley,    | 6.5             | 152 | 188 | 0.1    | 0.3 |
| LA3         | Landers, 1992       | 7.3             | 163 | 164 | 0.7    | 0.3 |
| LA4         | Kern, 1952          | 7.3             | 201 | 139 | 0.2    | 0.2 |
| LA5         | Loma Prieta, 1989   | 7               | 257 | 374 | 0.2    | 0.2 |
| LA6         | Northridge, 1994,   | 6.7             | 262 | 254 | 0.3    | 0.3 |
| LA7         | Northridge, 1994,   | 6.7             | 206 | 224 | 0.3    | 0.2 |
| LA8         | Northridge, 1994,   | 6.7             | 220 | 316 | 0.3    | 0.3 |
| LA9         | North Palm Springs, | 6               | 394 | 381 | 0.1    | 0.2 |
| LA10        | Coyote Lake, 1979   | 5.7             | 228 | 129 | 0.1    | 0.2 |
| LA11        | Morgan Hill, 1984   | 6.2             | 123 | 211 | 0.1    | 0.1 |
| LA12        | Parkfield, 1966,    | 6.1             | 301 | 244 | 0.3    | 0.3 |
| LA13        | Parkfield, 1966,    | 6.1             | 268 | 305 | 0.1    | 0.2 |
| LA14        | North Palm Springs, | 6               | 200 | 146 | 0.1    | 0.2 |
| LA15        | Whittier, 1987      | 6               | 297 | 185 | 0.7    | 0.2 |

critical damping for the horizontal components, scaled to  $S_d/g=1.0$  at a period of 1.03 s, are shown in Figs. 4(a) and 4(b), for the NS and EW directions, respectively.

The gravity loads are simultaneously applied with the seismic loads. The following gravity loads (FEMA 355C, 2000) are used in the analysis: (a) the floor dead load for weight calculations was 96 psf; (b) the floor dead load for mass calculations was 86 psf; (c) the roof dead load was 83 psf; (d) the reduced live load per floor and for roof was 20 psf. The seismic mass for the entire structure was as follow. For the 3-level building it was 70.90 kips-sec<sup>2</sup>/ft for the Roof and 65.53 kips-sec<sup>2</sup>/ft for Floors 2 and 3. For the 9-

level building it was 73.10 kips-sec<sup>2</sup>/ft for the Roof, 69.04 kips-sec<sup>2</sup>/ft for Floor 2 and 67.86 kips-sec<sup>2</sup>/ft for Floors 3 to 9. For the 20-level building it was 40.06 kips-sec<sup>2</sup>/ft, 38.63 kips-sec<sup>2</sup>/ft and 37.76 kips-sec<sup>2</sup>/ft, for the Roof, Floor 2, and Floors 3 to 20, respectively.

In order to have different levels of deformation, namely elastic, moderate inelastic, and significant inelastic behavior, the strong motions are scaled in terms of the spectral pseudo-acceleration evaluated at the fundamental vibration period of the structure ( $S_a(T_1)$ ). The values of  $S_a$  vary from 0.2 g to 1.2 g with increment of 0.2 g for the 3-level building; from 0.1 g to 0.5 g for the 9-level building, and from 0.1 g to 0.3 g for the 20-level building; in the last two cases the increment was of 0.1 g. Thus considering 3 building models, 15 strong motions, PP and SR connections, and 6, 5 and 3 levels of deformation, for the 3-, 9-, and 20-level buildings, respectively, about 1500 step by step nonlinear analyses of systems with several thousands of degrees of freedom were required. For the case of the 3-level building, the behavior is elastic in most of the cases for seismic intensities of 0.2 g and 0.3 g, moderate yielding occurs for 0.4 g and 0.5 g, but significant yielding is observed for 1.0 g and 1.2 g. The corresponding seismic intensities for the 9-level building are 0.1 g, 0.3 g and 0.5 g, while those of the 20-level building are 0.1 g, 0.2 g and 0.3 g. It is worth to mention that for the maximum intensities, a deformation state very close to collapse was developed for some strong motions; interstory drifts of about 5% were observed for a few particular cases.

4.5 Ductility definitions

As commented before, one of the main objectives of this

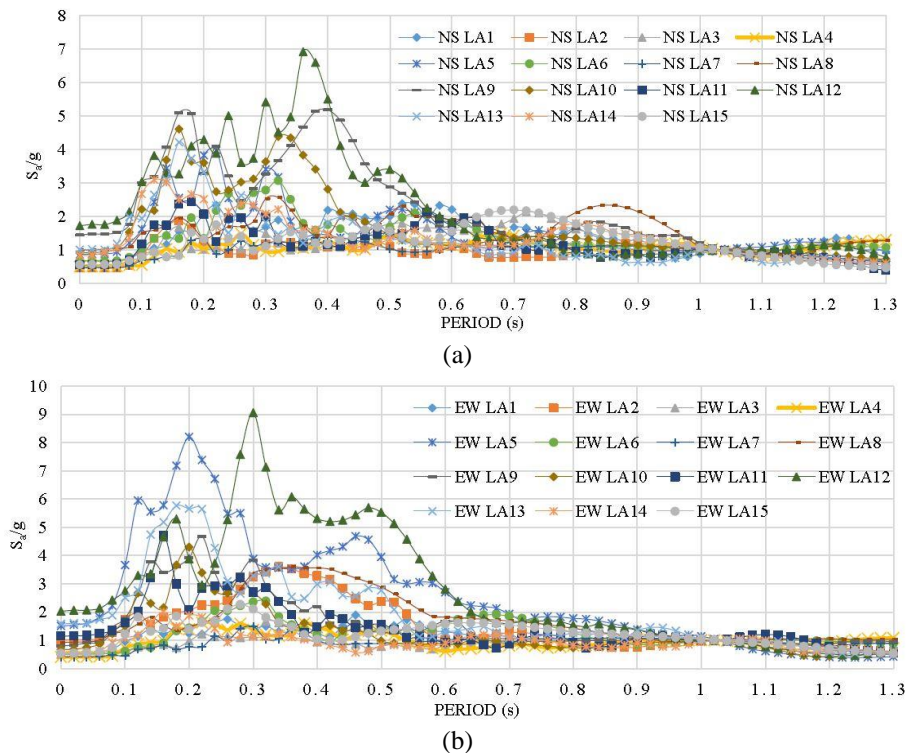


Fig. 4 Response spectra; (a) NS direction, (b) EW direction

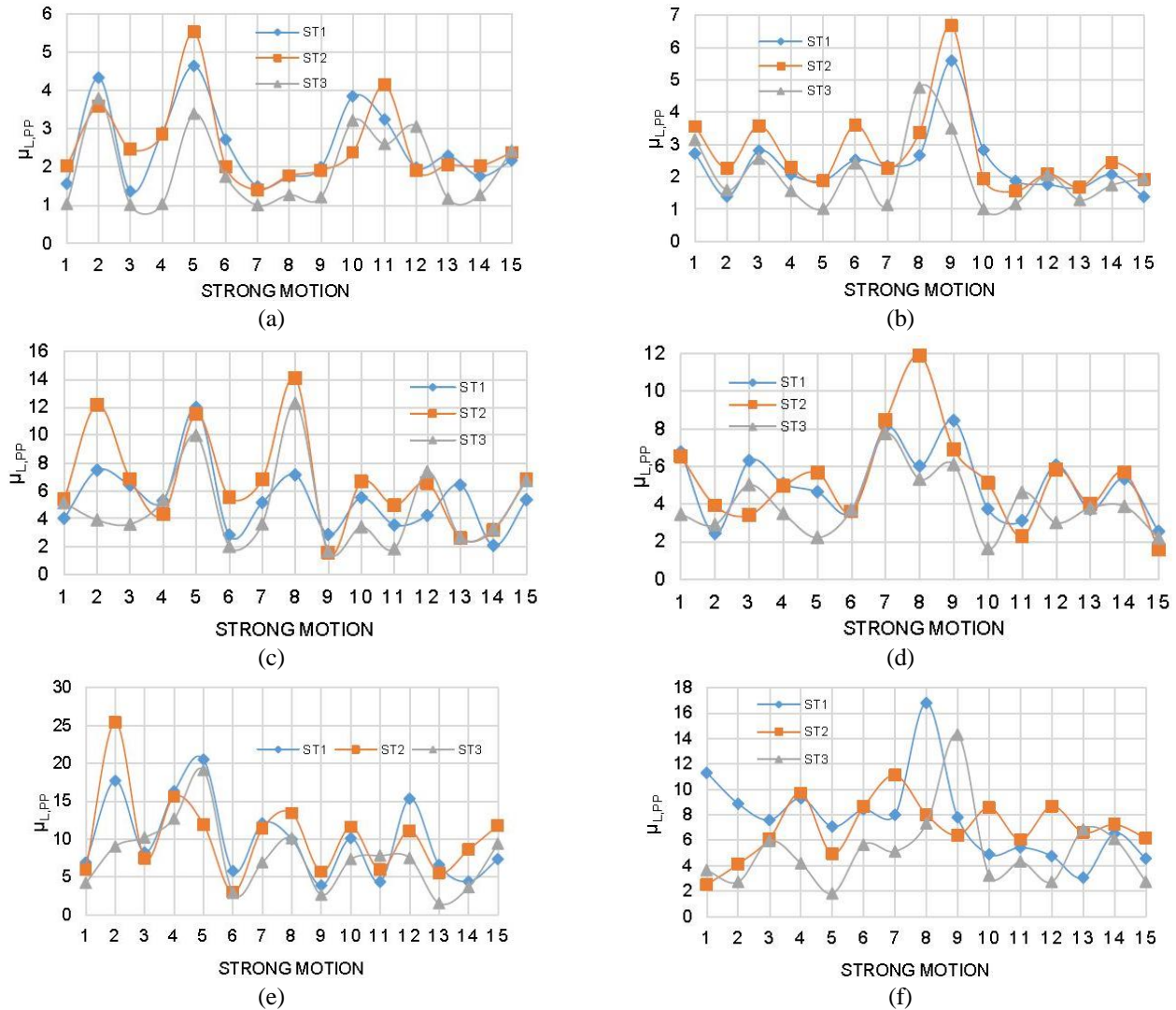


Fig. 5 Bending local ductility demands, the 3-level building with PP connections ( $\mu_{L,SR}$ ); (a)  $S_a=0.4$  g NS, (b)  $S_a=0.4$  g EW, (c)  $S_a=0.8$  g NS, (d)  $S_a=0.8$  g EW, (e)  $S_a=1.2$  g NS and (f)  $S_a=1.2$  g EW

paper is to evaluate the ductility demands (local and story) associated to deformations of steel buildings with interior PP and SR connections produced by the action of seismic loading. Conceptually, for SDOF systems, ductility is defined as the ratio of the maximum inelastic displacement ( $D_{max}$ ) to the yield displacement ( $D_y$ ).  $D_{max}$  is calculated as the maximum displacement that the system undergoes during the application of the total seismic loading and  $D_y$  as the displacement of the system when yielding occurs on it for the first time. For MDOF systems, however, it is not clearly stated how to calculate these two parameters ( $D_{max}$  and  $D_y$ ). Since global ductility should represent the overall structural inelastic deformation, some researchers suggest defining it in terms of relative lateral displacements (drifts) (Newmark and Hall 1982, Uang 1991a, Osman *et al.* 1995). In this regard a definition of story ductility in terms of drifts is adopted in this study, as described below.

#### 4.5.1 Local ductility

Since in framed structures plasticization of beams and columns is produced mainly by bending, local ductility is

defined in terms of curvatures. Local ductility of a flexural member ( $\mu_L$ ) for a given joint is defined as the ratio of the maximum inelastic curvature that the joint undergoes during the total time of excitation ( $\phi_{max}$ ) to the curvature of the joint when it yields for the first time ( $\phi_y$ ). Mathematically it is expressed as

$$\mu_L = \frac{\phi_{max}}{\phi_y} \quad (1)$$

Thus, in the case of nonlinear time history analysis, as soon as any of the joints of a given member yields for the first time, the corresponding curvature is identified as  $\phi_y$  for that particular member. In a similar manner the curvature is calculated at each time increment of the analysis and the largest one is identified as  $\phi_{max}$  for the member under consideration.

#### 4.5.2 Story ductility

The ductility of a story ( $\mu_s$ ) is defined as the ratio of the maximum inelastic drift of the story during the total time of excitation ( $\Delta_{max}$ ) to the drift of the story when any of its

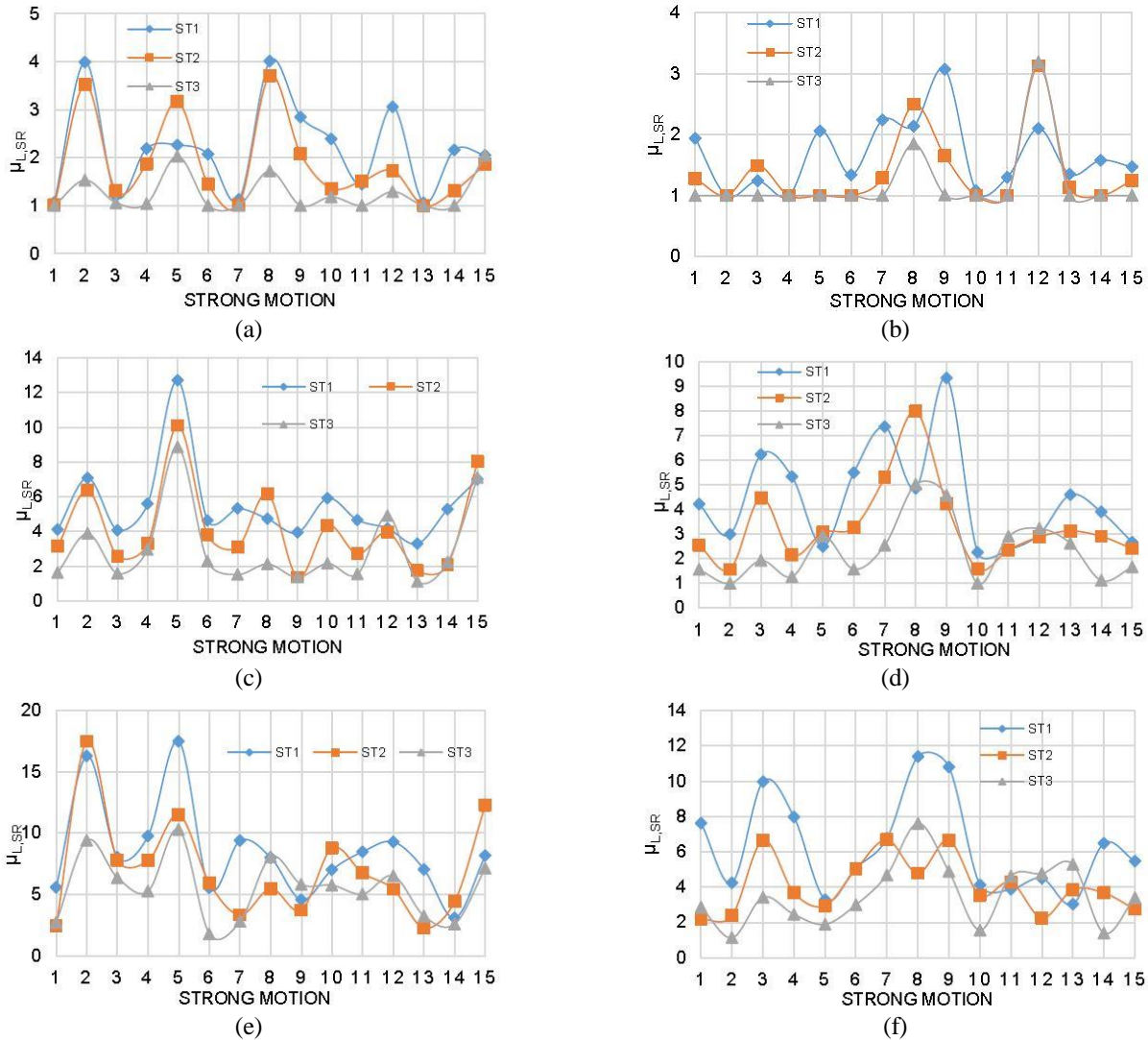


Fig. 6 Bending local ductility demands, the 3-level building with SR connections ( $\mu_{L,SR}$ ); (a)  $S_a=0.4$  g NS, (b)  $S_a=0.4$  g EW, (c)  $S_a=0.8$  g NS, (d)  $S_a=0.8$  g EW, (e)  $S_a=1.2$  g NS and (f)  $S_a=1.2$  g EW

members yields for the first time ( $\Delta_y$ ). Mathematically we have

$$\mu_S = \frac{\Delta_{max}}{\Delta_y} \tag{2}$$

It is assumed that for a given story of a given frame, the beams on the story and the columns connecting beneath it are part of the story. Then, in this definition, the expression “the drift of the story when any of its members yields for the first time” refers to first yielding of any beam or column that is part of the story under consideration; it will define the  $\Delta_y$  value for each story.

### 5. Ductility demands for the buildings with PP and SR connections

#### 5.1 Local ductility

The responses in terms of local ductility demands (Eq. (1)) are calculated for all beams and columns of the PMRF

of the three models under consideration for the above mentioned intensities of the 15 strong motions and the NS and EW directions. Because yielding did not occur in columns in most of the cases, particularly for low and moderate strong motion intensities, only the results for beams are reported. For a given story, the  $\mu_L$  values are averaged over all the beams of the story under consideration. The results for the 3-level model with PP connections ( $\mu_{L,PP}$ ) for the NS direction are shown in Figs. 5(a), 5(c), 5(e) for strong motions intensities of  $S_a=0.4$  g, 0.8 g and 1.2 g, respectively; the corresponding results for the EW direction are given in Figs. 5(b), 5(d) and 5(f). In these figures, the symbol “ST” defines the story level. It can be said that, for the 3-level building, the structural deformation produced by seismic intensities of 0.4 g and 0.8 g correspond to moderate (drift of about 1.5%) and significant yielding (drift of about 3%), respectively, while that of 1.2 g produces a deformation state close to the collapse; consequently it is associated to the structural capacity. The maximum drifts for largest level of deformation was about 5% for some of the strong motions

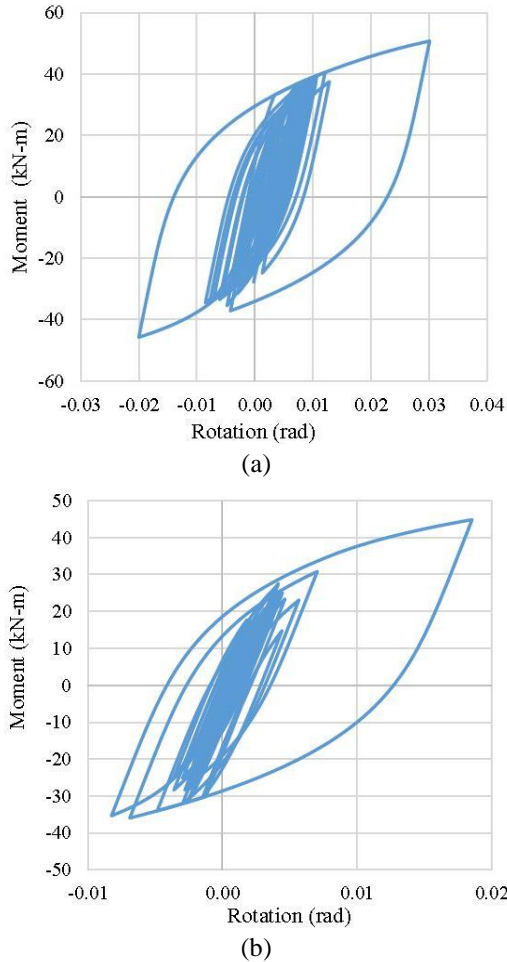


Fig. 7 Typical Moment-rotations curves for SR, NS PMRF, 3-level building, Strong Motion 4,  $S_a=0.8$  g, (a) First Story, (b) Second Story

and collapse mechanisms were observed in some cases. It is assumed in this paper that this level of deformation is associated the structural capacity of the models.

It is shown in Fig. 5 that, for a particular value of  $S_a$  and story, the magnitude of  $\mu_L$  significantly varies from one seismic motion to another reflecting the effect of the strong motion frequencies and of the contribution of several vibration modes. It is also shown that, as expected, the  $\mu_L$  values increase as the seismic intensity increases. The maximum value of  $\mu_L$  (bending local ductility capacity) associated to the greatest seismic intensity ( $S_a=1.2$  g) is larger than 16 in some cases; considering all stories and strong motions, the average value is about 12. It is worth to mention that, even not shown in the paper, the corresponding averages are a little larger for the taller buildings.

The local ductility demands for the 3-level building with SR connections ( $\mu_{L,SR}$ ) for the same intensities used in Figs. 5 (PP connections) are presented in Fig. 6. Most of the observations made for the model with PP connections apply to this case. The most important observation that can be made at this state is that the local ductility demands of the model with SR connections can be significantly smaller than those of the model with PP connections. The

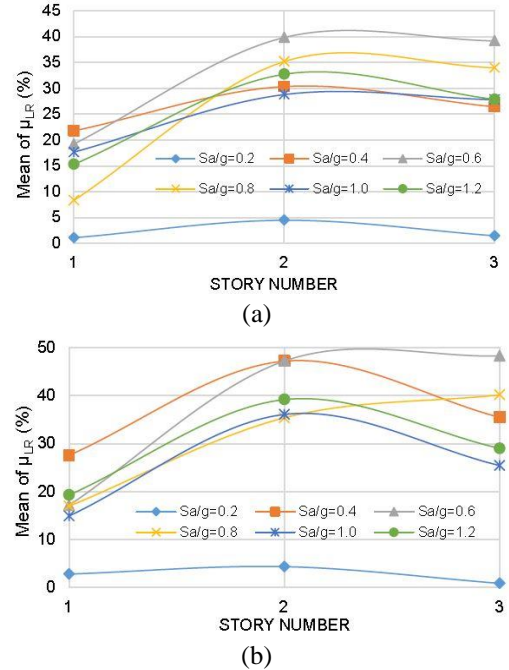


Fig. 8 Mean values of  $\mu_{LR}$  (%), 3-level building, (a) NS direction, (b) EW direction

magnitude of the reduction significantly varies from one strong motion to another and from one story level to another. For low seismic intensities, as expected, the reduction is practically null, however, for moderate or large seismic intensities it can be considerable; for example, for  $S_a=1.2$  g, Strong Motion 5 and NS direction (Fig. 5(e)) the local ductility demand for Story 3 is about 19 for the building with interior PP connections, while the corresponding value for the case of SR connections (Fig. 6(e)) is about 10. The implication of this is that modeling the connections in a more realistic way, i.e., as SR, helps to significantly reduce the local ductility demands at PMRF and so the structural damage. Typical moment-rotation curves corresponding to the connections of the PMRF oriented in the NS direction of the 3-level building for a seismic intensity of 0.8g for Strong Motion 5 are presented in Figs. 7(a) and 7(b), for the first and second story, respectively.

Graphs similar to those given in Figs. 5 and 6 were also developed for several other seismic intensities; in total 24 plots were developed for the 3-level building, but they are not shown. Similar sets of plots were also developed for the 9- and 20-level building. However, it is not possible to give all these results; only the fundamental statistics (calculated over all the strong motions) in terms of the mean value (MV) of the ductility demand reduction (in percent) are shown for all cases. Such reduction is calculated as

$$\mu_{LR} = \frac{(\mu_{L,PP} - \mu_{L,SR})}{\mu_{L,PP}} \times 100 \quad (3)$$

The mean values of  $\mu_{LR}$  for the 3-level model are presented in Figs. 8(a) and 8(b) for the NS and EW directions, respectively. As observed before from the plots of individual strong motions, the mean values of the local

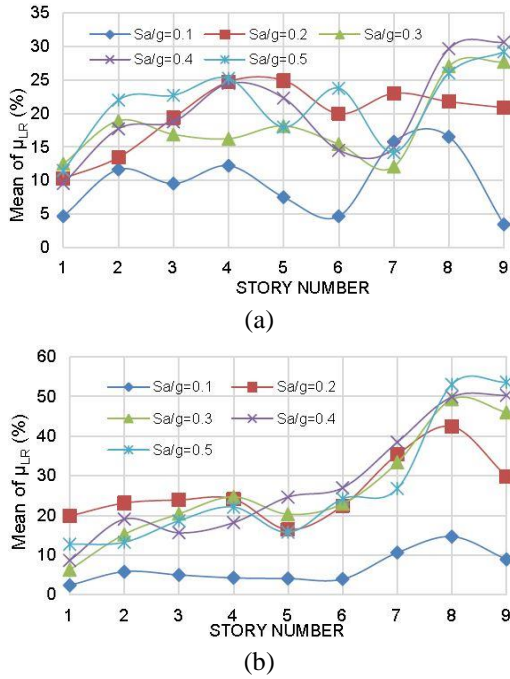


Fig. 9 Mean values of  $\mu_{LR}$  (%), 9-level building, (a) NS direction, (b) EW direction

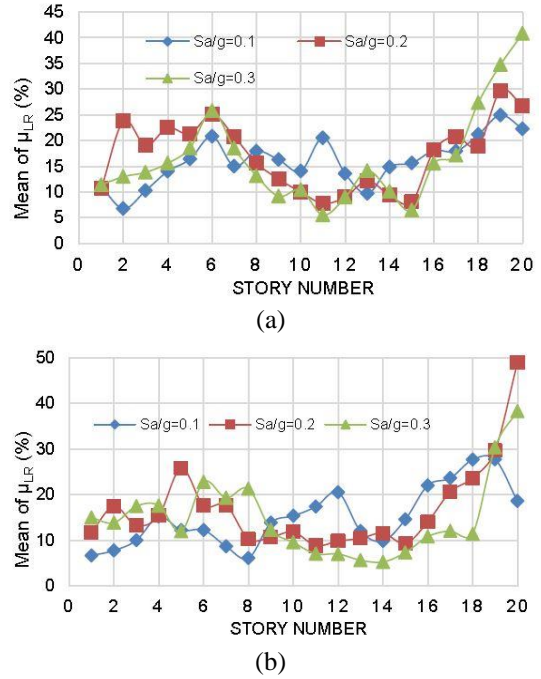


Fig. 10 Mean values of  $\mu_{LR}$  (%), 20-level building, (a) NS direction, (b) EW direction

ductility reduction is small for the lowest seismic intensity, but for the others it can be significant; the largest value occurs, in general, for Stories 2 and 3. Values larger than 40% are observed in many cases. No clear tendency is observed between the magnitude of the reduction and the intensity of the seismic motions. The values are quite similar for the NS and EW direction.

The results for the 9-level model are presented in Fig 9. Most of the observations made for the 3-level building apply to this model. The additional observation that can be made is that, unlike the 3-level building, the maximum mean values of  $\mu_{LR}$  are, in general, larger for the two upper stories and that they are larger for the EW than for the NS direction; values larger than 40% can be observed for Stories 8 and 9 for the EW direction. The results for the 20-level model are shown in Fig. 10. As for the case of the 9-level building the maximum values occurs for the two upper stories which are quite similar to the maximum ones of the 3- and 9-level model.

### 5.2 Story ductility

The story ductility demands (Eq. (2)) are now discussed. As for local ductility demands,  $\mu_S$  is calculated for the three models with PP and SR connections, for both horizontal directions, for each individual strong motion and several seismic intensities. However, only the mean values of the reduction produced by the effect of SR connections are presented. The reduction is calculated as

$$\mu_{SR} = \frac{(\mu_{S,PP} - \mu_{S,SR})}{\mu_{S,PP}} \times 100 \quad (4)$$

The terms in Eq. (4) have the same meaning as those in Eq. (3) but story ductility is calculated instead. The mean

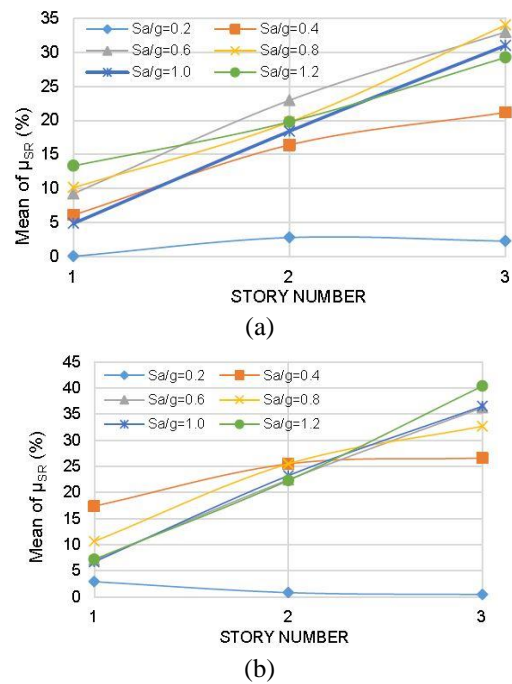
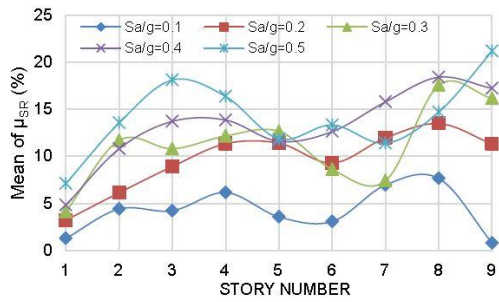
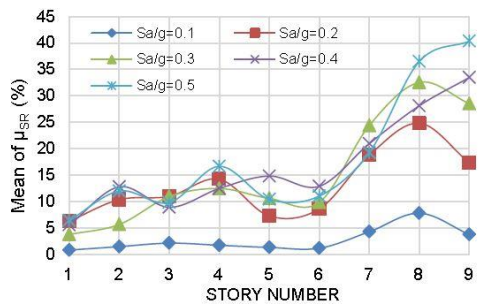


Fig. 11 Mean values of  $\mu_{SR}$  (%), 3-level building, (a) NS direction, (b) EW direction

values of  $\mu_{SR}$  are given in Figs. 11, 12 and 13, for the 3-, 9- and 20-level buildings, respectively. As for the case of local ductility demands, significant reductions are observed in story ductility demands when SR are considered in the interior gravity frames. For the case of the 3-level building the reduction reaches mean values larger than 30% in many cases and tend to linearly increase with the story number. For the 9-level building the reduction is also significant and, even though not in a perfect way, tend to increase with the

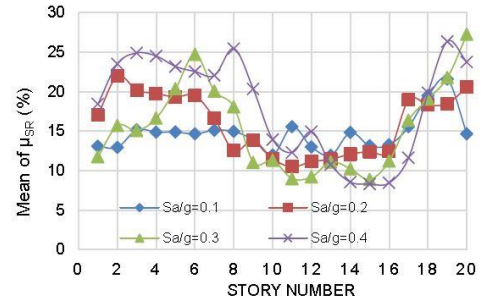


(a)

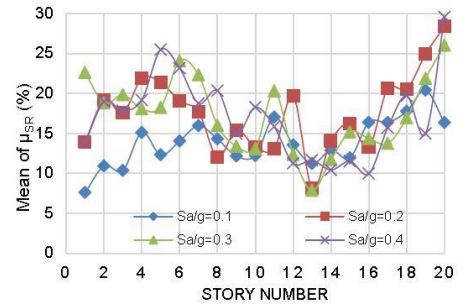


(b)

Fig. 12 Mean values of  $\mu_{SR}$  (%), 9-level building, (a) NS direction, (b) EW direction



(a)



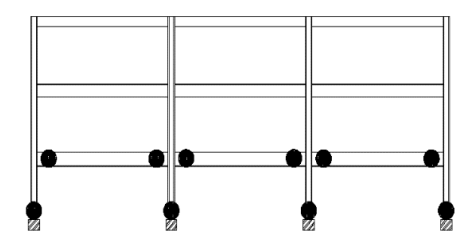
(b)

Fig. 13 Mean values of  $\mu_{SR}$  (%), 20-level building, (a) NS direction, (b) EW direction

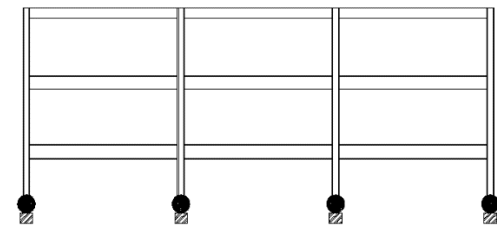
story number. This trend is not observed for the 20-level building; the reduction are larger, in general, for Stories 1 to 8 and for Stories 18 to 20 than for the others. By comparing local with story ductility reductions it is observed that they are smaller for the latter.

The earlier results clearly indicate that the local and story ductility demands on the PMRF are significantly reduced when the usually neglected effect of connections of the IGF are considered. One of the reasons for the ductility reduction demands is, as observed in some experimental investigations (Nader and Astaneh-Asl 1991, Leon and Shin 1995), the effect of the dissipated hysteretic energy at SR connections. The implication of this is that the behavior of

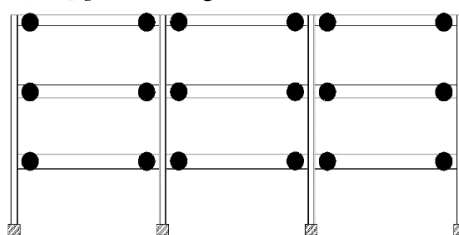
the model with SR connections is superior to that of PP connections since a much smaller structural damage is expected to occur. In addition, the ductility detailing of the PMRF doesn't need to be so stringent when the effects of SR connections are considered. The maximum number of plastic hinges developed in the PMRF of the 3-level building for the NS direction for two particular strong motions (Strong motions 4 and 8) is presented in Fig. 14. The percent of reductions in the story ductility demand are about 18% and 28% for Strong Motions 4 and 8, respectively. As observed in the figure, the number of plastic hinges is significantly reduced when the connections are modeled as SR.



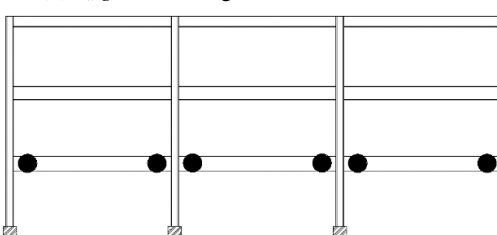
(a)  $S_d/g=1.0$ , Strong Motion 4, PP connection



(b)  $S_d/g=1.0$ , Strong Motion 4, SR connection



(c)  $S_d/g=1.0$ , Strong Motion 8, PP connection



(d)  $S_d/g=1.0$ , Strong Motion 8, SR connection

Fig. 14 Maximum number of plastic hinges

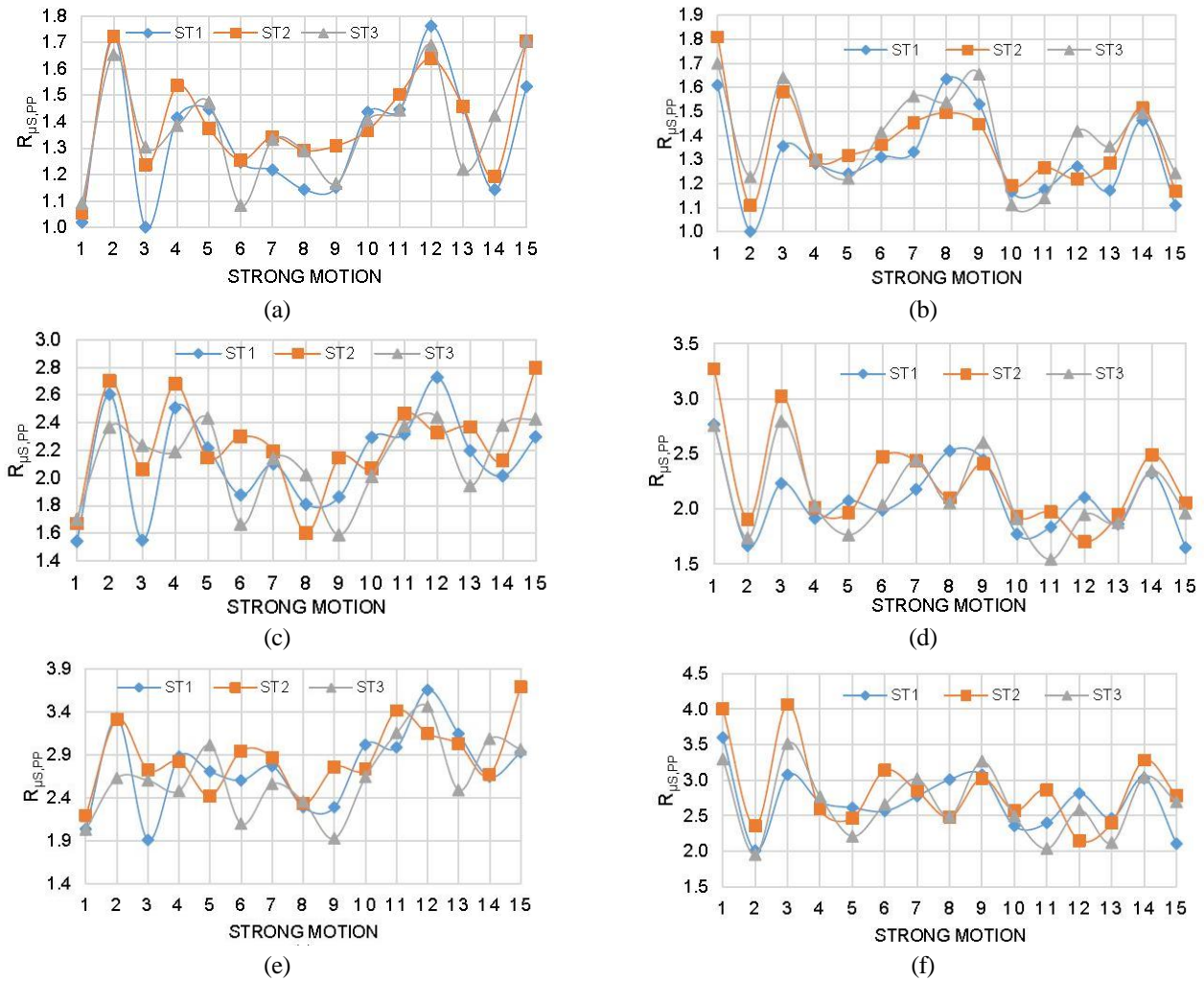


Fig. 15  $R_{\mu S,PP}$ , 3-level building; (a)  $S_a = 0.4$  g NS, (b)  $S_a = 0.4$  g EW, (c)  $S_a = 0.8$  g NS, (d)  $S_a = 0.8$  g EW, (e)  $S_a = 1.2$  g NS, (f)  $S_a = 1.2$  g EW

### 6. Results in terms of ductility reduction factors

The story ductility reduction factor ( $R_{\mu S}$ ) is calculated as

$$R_{\mu S} = \frac{V_e}{V_i} \tag{5}$$

where for a given story of a PMRF,  $V_e$  represents the total base shear considering the contribution of all columns at the story obtained from an elastic analysis (yielding is not allowed in the structure) and  $V_i$  represents the same but obtained from an inelastic analysis. Similar to the case of  $\mu_S$ ,  $R_{\mu S}$  is calculated for all stories of the three building models under consideration, for both horizontal directions and several intensities of the fifteen strong motions, as well as for PP and SR connections.

Typical results are given in Fig. 15 for the 3-level building with PP connections ( $R_{\mu S,PP}$ ). It can be seen that the  $R_{\mu S,PP}$  values significantly vary from one strong motion to another and from one story to another even though in the Equivalent Static Lateral Method (ESLM) the reduction is assumed to be the same for any story. Results for  $R_{\mu S,PP}$  were also developed for several other seismic intensities of the 3-level building as well as for the 9- and 20-level

building, but only the mean values are shown for all cases; they are presented in Figs. 16, 17 and 18, for the 3-, 9- and 20-level models, respectively. It can be seen that, as expected, the mean values of  $R_{\mu S,PP}$  significantly increase with the strong motion intensity. The reason for this is that the elastic ( $V_e$  in Eq. (5)) and the inelastic ( $V_i$  in Eq. (5)) interstory shears are very close each other for small levels of deformation (small  $S_a$ ); for large deformations, however,  $V_e$  increases linearly with  $S_a$  but,  $V_i$  does not. Most importantly, for the 3-level building the values are approximately constant for the three stories, while for the 9-level they are approximately constant for the first four stories, they tend to increase for the following four stories with the increment ratio being larger for larger  $S_a$  values, and finally decrease for the upper story. The  $R_{\mu S,PP}$  mean values of the 20-story building resemble those of the 9-story building in the sense that they are closely constant for the first five stories, but they tend to increase for the following thirteen stories and tend to decrease for the last two stories.

According to the ESLM, interstory shears, bending moments and axial forces are reduced in the same proportion regardless the story number. The results of this study indicate, however, that this “same proportion

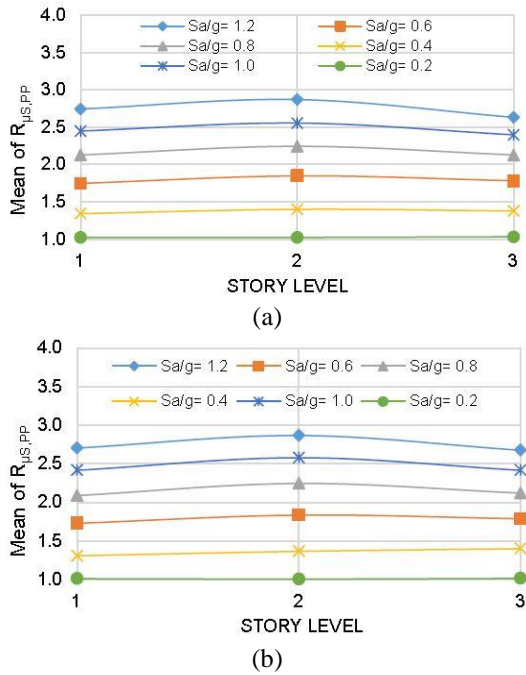


Fig. 16 Mean values of  $R_{\mu S,PP}$ , 3-level building, (a) NS Direction, (b) EW Direction

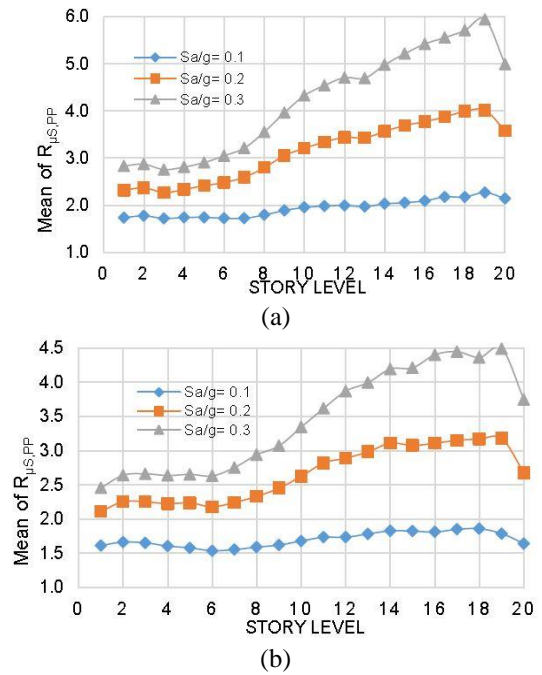


Fig. 18 Mean values of  $R_{\mu S,PP}$ , 20-level building, (a) NS Direction, (b) EW Direction

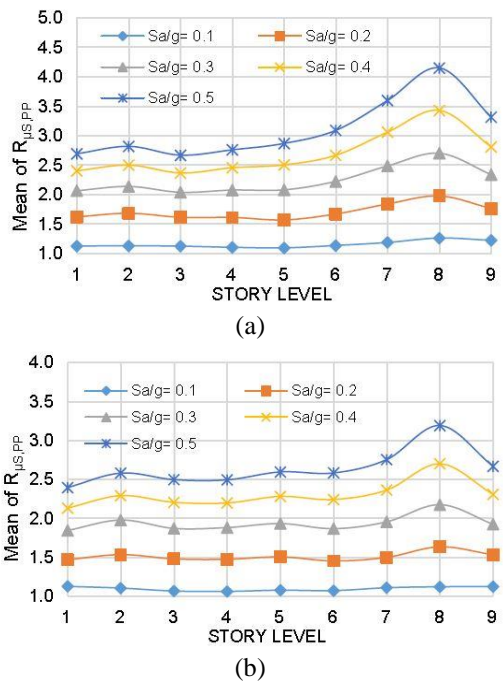


Fig. 17 Mean values of  $R_{\mu S,PP}$ , 9-level building, (a) NS Direction, (b) EW Direction

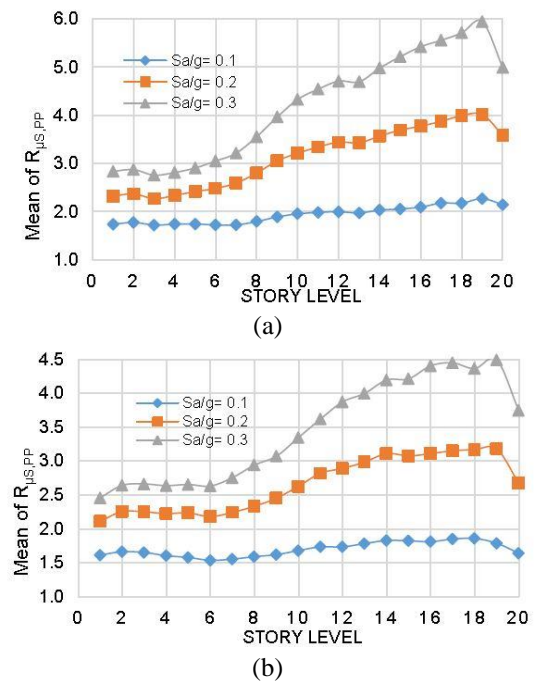


Fig. 19 Mean values of  $Q_{SL}$ , 3-level building, (a) NS Direction, (b) EW Direction

reduction” is only valid for the 3-level building; as stated above it reflects an important limitation of the ESLM where the ductility reduction factor does not depend on the story height. For the case of the largest seismic intensities ( $S_a=1.2$  g, 0.5 g and 0.3 g for the 3-, 9- and 20-level buildings respectively), which are associated to the ductility capacity, the mean values ranges from 2.6 to 2.9, from 2.4 to 4.2 and from 2.5 to 5.9 for the 3-, 9-, and 20-level models, respectively. In addition in seismic codes like International

Building Code, it is implicitly assumed that the overall ductility reduction factor for ductile moment resisting frames is about 4; the results of this study indicate that this value is non conservative for the 3-level building or for the lower stories of the 9- and 20-level building. For the upper stories of the 9- and 20-level buildings, however, values of up to 6 are observed, implying conservative designs. The implication of this is, again, that the ESLM fails evaluating the inelastic interstory shears in the upper stories of mid-

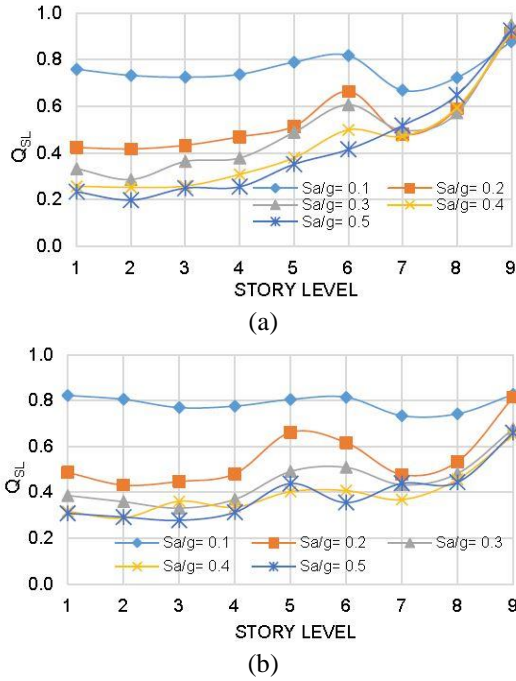


Fig. 20 Mean values of  $Q_{SL}$ , 9-level building, (a) NS Direction, (b) EW Direction

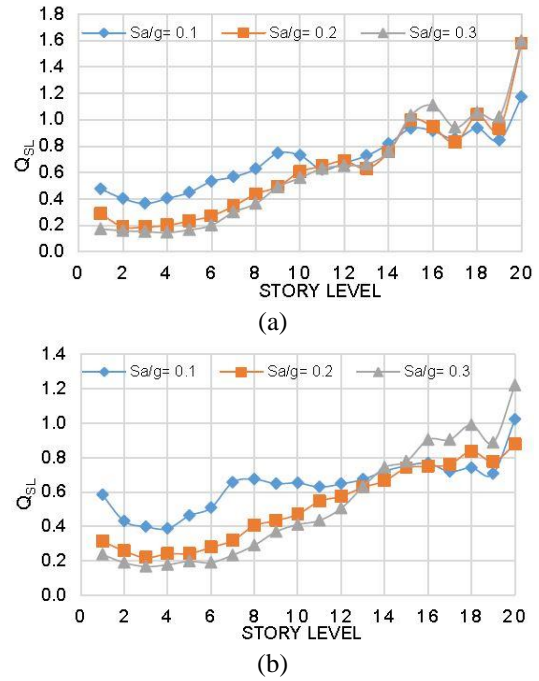


Fig. 21 Mean values of  $R_{SL}$ , 20-level building, (a) NS Direction, (b) EW Direction

and high-rise buildings.

It is worth to mention that the significant reduction of the interstory shears of the upper stories in many cases is not due to the fact that significant yielding occurred in those stories, but it is due to significant yielding occurred in stories of the medium and low part of the structure. The implication of this is that yielding on a certain part of the structure produce reduction of the interstory shear not only on that part but also in other parts of the structure even if they remain elastic. This important result cannot be observed in buildings with a few stories like the 3-level buildings and even less in structures modeled as SDOF systems.

The results for the models with SR connections ( $R_{\mu G,SR}$ ) were also calculated but they are not shown. It is worth to mention that, in general, they are smaller than those of  $R_{\mu G,PP}$ . However, the individual components in Eq. (5) ( $V_e$  and  $V_i$ ) are significantly smaller for the frames with SR connections, which implies that the elastic or inelastic interstory shears of the PMRF are greatly reduced when the connections are modeled as SR.

### 7. Ratio of ductility reduction factor to local ductility

If local ductility is stated as the basis for design, as discussed in Section 1 of the paper, it is important to establish a relationship between  $R_{\mu S}$  and  $\mu_L$ . This relation ( $Q_{SL}$ ) is calculated as

$$Q_{SL} = \frac{R_{\mu S}}{\mu_L} \tag{6}$$

The values of  $Q_{SL}$ , as for the response parameters presented before, are calculated for each individual strong

motion but only the mean values of the models with PP connections are discussed; they are given in Figs. 19, 20 and 21 for the 3-, 9- and 20-level buildings, respectively.

Results indicate that, in general, the mean values of  $Q_{SL}$  tend to decrease with the seismic intensity but the decrement ratio is smaller for the upper stories; in fact for the 20-story model the variation from one  $S_a$  value to another is much smaller for Stories 12 to 20 than for Stories 1 to 11. It is also observed that the mean values of  $Q_{SL}$ , in general, tend to increase with the story number, which is more significant for the higher buildings.

For the case of deformation state close to collapse ( $S_d/g=1.2, 0.5$  and  $0.3$ , for the 3-, 9- and 20-level building, respectively), the  $Q_{SL}$  mean values are about 0.3 for the first two stories and a little larger for the upper story of the 3-level building, while for the 9-level building they are about 0.3 for the first four stories, but larger than 0.5 in many case for the last three st, but larger than 0.7 for many cases of the last four stories. If local ductility capacity is stated as the basis for design, and if it is assumed that the average value of 12 mentioned earlier is reasonable,  $Q_{SL}$  mean values of about 0.3 will indicate that the story ductility reduction factor will be about 3.6. However, a  $Q_{SL}$  mean value of 0.8 indicate that the story ductility reduction factor is about 9.6 which is much larger than the implicitly assumed value of 4 in the International Building Code. The implication of this is, as stated above, that the interstory shears acting upon the upper stories, particularly for the 9- and 20-level building models, calculated according to the ESLM are overestimated resulting in conservative designs.

In order to propose a value of the  $Q_{SL}$  ratio based on the results of this study, the values of the  $Q_{SL}$  parameter are averaged over all the stories giving the overall ratio ( $Q_{GL}$ ) of ductility reduction factor to local ductility. The resulting

values are 0.38, 0.41 and 0.57 for the 3-, 9- and 20-level buildings, respectively. Thus a value of 0.4 seems to be reasonable for low- and mid-rise buildings; for the case of high-rise buildings, even though the ESLM may not be applicable, a value of 0.6 would be appropriate.

## 8. Conclusions

The results of a numerical investigation regarding the ductility demand evaluation of steel buildings with perimeter moment resisting frames (PMRF) and interior gravity frames (IGF), considering the connections, firstly as perfectly pinned (PP), and then in a more realistic way, i.e., as semi-rigid (SR), are presented in this study. Three models used in the SAC steel project, representing steel buildings of low-, mid- and high-rise, as well as 15 strong motion records, are considered in the study. Local ( $\mu_L$ ) and story ( $\mu_S$ ) ductility demands are calculated for the PMRF for the buildings with the idealized PP connections and are compared with those obtained for the more accurate representation (SR) of the connections. The story ductility reduction factor ( $R_{\mu_S}$ ) as well as the ratio ( $Q_{GL}$ ) of  $R_{\mu_S}$  to  $\mu_L$  are also calculated. Based on the results of the study the following conclusions are made:

(1) Local ductility demands at the PMRF are significantly reduced when the usually neglected effect of the SR connections of the IGF are considered. Average reductions larger than 40% are observed in many cases. One of the reasons for such reduction is that, as observed in experimental investigations, SR connections introduce an important source of energy dissipation. The implication of this is that the behavior of the models with SR connections is superior to that of PP connections since smaller structural damage occurs. In addition, the ductility detailing of the PMRF does not need to be so stringent when the effect of SR is taken into account. As for the case of  $\mu_L$ , significant reductions are observed for  $\mu_S$  when SR are considered; reductions larger than 30% are observed in many cases. For the case of the 3-level building the reductions tend to linearly increase with the story number, while for the 9- and 20-level buildings are, in general, larger for the 3 upper stories.

(2) The mean values of  $R_{\mu_S}$  significantly increase with the strong motion intensity. For the 3-level building, the values are approximately constant for the three stories, but for the 9- and 20-level buildings they tend to, in general, increase with the story number. According to the Equivalent Static Lateral Method (ESLM) interstory shears are reduced in the same proportion regardless the story number. The results of this study indicate, however, that this same proportion reduction is only valid for the 3-level building, reflecting an important limitation of the ESLM. In seismic codes like International Building Code, it is implicitly assumed that the overall ductility reduction factor for ductile moment resisting frames is about 4; the study shows that this value is non-conservative for the 3-level building, or for the lower stories of the 9- and 20-level building,

however, it is conservative for the upper stories of the 9- and 20-level buildings. The implication of this is that the ESLM fails evaluating the inelastic interstory shears of the upper stories of mid- and high-rise buildings.

(3) For the case of deformation state close to collapse, the mean values of the  $Q_{SL}$  ratio for the 3-level building are about 0.3 for the first two stories and a little larger for the upper story. For the 9-level building they are about 0.3 for the first four stories but larger than 0.5 in many case for the last three stories, values of up to 0.6 are observed. For the 20-level building they are about 0.2 for the first eight stories but larger than 0.7 for many cases for the last four stories. If local ductility capacity is stated as the basis for design, and if it is assumed that an average value of 12 is reasonable,  $Q_{SL}$  mean values of about 0.3 will indicate that the story ductility reduction factor will be about 3.5, which is not conservative. However, a  $Q_{SL}$  mean value of 0.8 indicate that the story ductility reduction factor is about 9.5 which is much larger than the value of 4 implicitly assumed in the International Building Code. The implication of this is that, as stated above, the interstory shears acting upon the upper stories, particularly for the 9- and 20-level building models, calculated according to the ESLM are overestimated resulting in conservative designs.

(4) In order to propose a value of the  $Q_{SL}$  ratio based on the results of this study, the values of the  $Q_{SL}$  parameter are averaged over all the stories giving the overall ratio ( $Q_{GL}$ ) of ductility reduction factor to local ductility. The resulting values are 0.38, 0.41 and 0.57 for the 3-, 9- and 20-level buildings, respectively. Thus a value of 0.4 seems to be reasonable for low- and mid-rise buildings; for the case of high-rise buildings, even though the ESLM may not be applicable, a value of 0.6 would be appropriate.

(5) The findings of this paper were based on the particular models and strong motions used in the study. More research is needed to reach more general conclusions.

## Acknowledgements

This paper is based on work supported by La Universidad Autónoma de Sinaloa (UAS) under grant PROFAPI-2015/235. Financial support from The Universidad Nacional Autónoma de Mexico (PAPIIT IN103517) is also appreciated. Any opinions, findings, conclusions, or recommendations expressed in this publication are those of the authors and do not necessarily reflect the views of the sponsors.

## References

- Abdi, H., Hejazi, F., Saifulnaz, R., Karim, I.A. and Jaafar, M.S. (2015), "Response modification factor for steel structure equipped with viscous damper device", *Int. J. Steel Struct.*, **15**(3), 605-622.
- Abdollahzadeh, G. and Banihashemi, M. (2013), "Response modification factor of dual moment-resistant frame with buckling restrained brace (BRB)", *Steel Compos. Struct.*, **14**(6), 621-636.
- Abdollahzadeh, G. and Faghihmaleki, H. (2014), "Response modification factor of SMRF improved with EBF and BRBs", *J.*

- Adv. Res. Dyn. Control Syst.*, **6**(4), 42-55.
- Arroyo-Espinoza, D. and Teran-Gilmore, A. (2003), "Strength reduction factors for ductile structures with passive energy dissipating devices", *J. Earthq. Eng.*, **7**(2), 297-325.
- ATC (Applied Technology Council) (1978), "Tentative provisions for the development of seismic regulation buildings", Report No. ATC-3-06, Redwood City, California.
- Ayoub, A. and Chenouda, M. (2009), "Response spectra of degrading structural systems", *Eng. Struct.*, **31**, 1393-1402.
- Bayat, M. and Zahrai, S.M. (2017), "Seismic performance of mid-rise steel frames with semi-rigid connections having different moment capacity", *Steel Compos. Struct.*, **25**(1), 1-17.
- Borzi, B. and Elnashai, A.S. (2000), "Refined force reduction factors for seismic design", *Eng. Struct.*, **22**, 1244-1260.
- Cai, J., Zhou, J. and Fang, X. (2006), "Seismic ductility reduction factors for multi-degree-of-freedom systems", *Adv. Struct. Eng.*, **9**(5), 591-601.
- Carr, A. (2011) "RUAUMOKO, Inelastic dynamic analysis program", Ph.D. Dissertation, University of Cantenbury, Cantenbury, England.
- Chen, W.F. and Atsuta, T. (1971), "Interaction equations for biaxially loaded sections", Fritz Laboratory Report (72-9), Lehigh University, Paper 284.
- Chopra, A.K. (2008), *Dynamics of Structures*, Prentice Hall, New Jersey, USA.
- Disque, R.O. (1964), "Wind connections with simple framing", *Eng. J.*, AISC, **1**(3), 101-103.
- Elnashai, A.S. and Elgazhouli, A.Y. (1994), "Seismic behavior of semi-rigid steel frames", *J. Constr. Steel Res.*, **29**(1-3), 149-174.
- Elnashai, A.S. and Mwafy, A.M. (2002), "Overstrength and force reduction factors of multistorey reinforced-concrete buildings", *Struct. Des. Tall Build.*, **11**, 329-351.
- Elnashai, A.S., Elghazouli, A.Y. and Denesh-Ashtiani, F.A. (1998), "Response of semi-rigid steel frames to cyclic and earthquake loads", *J. Struct. Eng.*, **124**(8), 857-867.
- FEMA (2000), State of the Art Report on Systems Performance of Steel Moment Frames Subject to Earthquake Ground Shaking, SAC Steel Project FEMA-355C, Federal Emergency Management Agency.
- Ganjavi, B. and Hao, H. (2012), "Effect of structural characteristics distribution of strength demand and ductility reduction factor of MDOF systems considering soil-structure interaction", *Earthq. Eng. Eng. Vib.*, **11**, 205-220.
- Gholipour, M., Mojtahedi, A. and Nourani, V. (2015) "Effect of semi-rigid connections in improvement of seismic performance of steel moment-resisting frames", *Steel Compos. Struct.*, **19**(2), 467-484.
- Hadianfard, M.A. (2012) "Using integrated displacement method to time-history analysis of steel frames with nonlinear flexible connections", *Struct. Eng. Mech.*, **41**(5), 675-689.
- Hadianfard, M.A. and Razani, R. (2003), "Effects of semi-rigid behavior of connections in the reliability of steel frames", *Struct. Saf.*, **25**(2), 123-138.
- Hadjian, A.H. (1989), "An evaluation of the ductility reduction factor Q in the 1976 regulations for the federal district of Mexico", *Earthq. Eng. Struct. Dyn.*, **18**, 217-231.
- Hetao, H. and Bing, Q. (2016), "Influence of cumulative damage on seismic response modification factors of elastic perfectly plastic oscillators", *Adv. Struct. Eng.*, **19**(9), 473-487.
- Karavasilis, T.L., Bazeos, N. and Beskos, D.E. (2008), "Drift and ductility estimates in regular steel MRF subjected to ordinary ground motions: A Design-Oriented approach", *Earthq. Spectra*, **24**(2), 431-451.
- Karmakar, D. and Gupta, V.K. (2006), "A parametric study of strength reduction factors for elasto-plastic oscillators", *Sadhana*, **31**(4), 343-357.
- Kartal, M.E., Basaga, H.B., Bayraktar, A. and Muvafik, M. (2010), "Effects of semi-rigid connection on structural responses", *Elec. J. Struct. Eng.*, **10**, 22-35.
- Kishi, N., Chen, F., Goto, Y. and Matsuoka, K.G. (1993), "Design aid of semi-rigid connections for frame analysis", *Eng. J., Am. Inst. Steel Constr.*, **30**, 90-107.
- Leon, R.T. and Shin, K.J. (1995), "Performance of semi-rigid frames", *Proceedings of Structures XIII Congress ASCE*, New York USA.
- Levy, R., Rutenberg, A. and Qadi, Kh. (2006), "Equivalent linearization applied to earthquake excitations and the R- $\mu$ -To relationships", *Eng. Struct.*, **28**(2), 216-228.
- Liu, Y. (2010), "Semi-rigid connection modeling for steel frameworks", *Struct. Eng. Mech.*, **35**(4), 431-547.
- Liu, Y. and Lu, Z. (2014), "Seismic behavior of suspended building structures with semi-rigid connections", *Earthq. Struct.*, **7**(4), 415-448.
- Miranda, E. and Bertero, V. (1994), "Evaluation of strength reduction factors for earthquake-resistant design", *Earthq. Spectra*, **10**(2), 357-379.
- Mohsenian, V. and Mortezaei, A. (2018), "Evaluation of seismic reliability and multi level response reduction factor (R factor) for eccentric braced frames with vertical links", *Earthq. Struct.*, **14**(6), 537-549.
- Nader, M.N. and Astaneh-Asl, A. (1991), "Dynamic behavior of flexible, semi-rigid and rigid frames", *J. Constr. Steel Res.*, **18**, 179-192.
- Nassar, A. and Krawinkler, H. (1991), "Seismic demands of SDOF and MDOF systems", Research Report No. 95, John A. Blume Earthquake Engineering Center, Stanford University.
- Newmark, N.M. and Hall, W.J. (1982), "Earthquake spectra and design monograph series", Earthquake Engineering Research Institute, Berkeley, California, USA.
- Ordaz, M. and Pérez-Rocha, L.E. (1998), "Estimation of strength-reduction factors for elasto-plastic systems: a new approach", *Earthq. Eng. Struct. Dyn.*, **27**(9), 889-901.
- Osman, A., Ghobarah, A. and Korol, M.R. (1995), "Implications of design philosophies of seismic response of steel moments frames", *Earthq. Eng. Struct. Dyn.*, **24**, 1237-143.
- Osteraas, J.D. and Krawinkler, H. (1990), "Strength and ductility considerations in seismic design", Research Report No. 90, Blume Earthquake Engineering Center, Stanford University.
- Reyes-Salazar, A. (2002), "Ductility and ductility reduction factors", *Struct. Eng. Mech.*, **13**(4), 369-385.
- Reyes-Salazar, A. and Haldar, A. (1999), "Nonlinear seismic response of steel structures with semi-rigid and composite connections", *J. Constr. Steel Res.*, **51**, 37-59.
- Reyes-Salazar, A. and Haldar, A. (2000), "Dissipation of energy in steel frames with PR connections", *Struct. Eng. Mech.*, **9**(3), 241-256.
- Reyes-Salazar, A. and Haldar, A. (2001a), "Energy dissipation at PR frames under seismic loading", *J. Struct. Eng.*, ASCE, **127**(5), 588-593.
- Reyes-Salazar, A. and Haldar, A. (2001b), "Seismic response and energy dissipation in partially restrained and fully restrained steel frames: An analytical study", *Steel Compos. Struct.*, **1**(4), 459-480.
- Reyes-Salazar, A., Bojorquez, E., Lopez-Barraza, A., Leon-Escobedo, D. and Haldar, A. (2009), "Some issues regarding the structural idealization of perimeter moment-resisting steel frames", *ASET J. Earthq. Technol.*, **46**(3-4), 133-146.
- Reyes-Salazar, A., Bojórquez, E., Velazquez-Dimas, J.I., López-Barraza, A. and Rivera-Salas, J.L. (2015), "Ductility and ductility reduction factors for steel buildings considering different structural representations", *Bull. Earthq. Eng.*, **13**(6), 1749-1771.
- Reyes-Salazar, A., Cervantes-Lugo, J.A., Lopez-Barraza, A., Bojorquez, E. and Bojorquez, J. (2016), "Seismic response of

- 3D Steel buildings with hybrid connections: PRC and FRC”, *Steel Compos. Struct.*, **22**(1), 113-139.
- Reyes-Salazar, A., Soto-López, M.E., Bojórquez, E. and López-Barraza, A. (2012), “Effect of modeling assumptions on the seismic behavior of steel buildings with perimeter moment frames”, *Struct. Eng. Mech.*, **41**(2), 183-204.
- Richard, R.M. (1993), “Moment-rotation curves for partially restrained connections”, PRCONN, RMR Design Group, Tucson, Arizona.
- Richard, R.M. and Abbott, B.J. (1975), “Versatile elastic plastic stress-strain formula”, *ASCE J. Eng. Mech.*, **101**(4), 511-515.
- Rupakhety, R. and Sigbjörnsson, R. (2009), “Ground-motion prediction equations (GMPEs) for inelastic displacement and ductility demands of constant-strength SDOF systems”, *Bull. Earthq. Eng.*, **7**, 661-679.
- Santa-Ana, P. and Miranda, E. (2000), “Strength reduction factors of multi-degree-of-freedom systems”, *12th World Conference on Earthquake Engineering*, Paper 1446, Auckland, New Zealand.
- Serror, M.H., Diab, R.A. and Mourad, S.A. (2014), “Seismic force reduction factor for steel moment resisting frames with supplemental viscous dampers”, *Earthq. Struct.*, **7**(6), 1171-1186.
- Shooshtari, A., Moghaddam, S.H. and Masoodi, A.R. (2015), “Pushover analysis of gabled frames with semi-rigid connections”, *Steel Compos. Struct.*, **18**(6), 1557-1568.
- Uang, C.M. (1991), “Establishing  $R$  (or  $R_u$ ) and  $C_d$  factors for building seismic provisions”, *J. Struct. Eng.*, ASCE, **117**(1), 19-28.
- Uang, C.M. (1991), “Structural overstrength and limit state philosophy in seismic design provisions”, Research Report No CE-91-0, Department of Civil Engineering, Northeastern University.
- Uang, C.M. and Bruneau, M. (2018), “State-of-the-art review on seismic design of steel structures”, *J. Struct. Eng.*, ASCE, **144**(4).
- UBC (1997), Structural Engineering Design Provisions; International Conference of Building Officials.
- Valipour, H.R. and Bradford, M.A. (2013), “Nonlinear  $P$ - $\Delta$  analysis of steel frames with semi-rigid connections”, *Steel Compos. Struct.*, **14**(1), 1-20.
- Whittaker, A., Hart, G. and Rojahn, C. (1999), “Seismic response modification factors”, *J. Struct. Eng.*, **125**(4), 438-444.

|                |                                                                      |
|----------------|----------------------------------------------------------------------|
| MRF            | Moment resisting frames                                              |
| FR             | Fully restrained                                                     |
| DWA            | Double web angles                                                    |
| PGA            | Peak ground accelerations                                            |
| $D_{max}$      | Maximum inelastic displacement                                       |
| $D_y$          | Yield displacement                                                   |
| $\phi_{max}$   | Maximum inelastic curvature                                          |
| $\phi_y$       | Curvature of a joint when it yields for the first time               |
| $\Delta_{max}$ | Maximum inelastic drift of the story                                 |
| $\Delta_y$     | Drift of the story when any of its members yields for the first time |
| $\mu_{L,PP}$   | Local ductility for the models with PP connections                   |
| $\mu_{L,SR}$   | Local ductility for the models with SR connections                   |
| $\mu_{LR}$     | Reduction in percentage of local ductility                           |
| $\mu_{SR}$     | Reduction in percentage of Story ductility                           |
| $R_{\mu S,PP}$ | Story Ductility Reduction Factor for the models with PP connections  |
| $R_{\mu G,PP}$ | Global Ductility Reduction Factor for the models with PP connections |

CC

## Abbreviations

### Symbol Definition

|             |                                              |
|-------------|----------------------------------------------|
| $\mu_L$     | Local ductility                              |
| $\mu_S$     | Story ductility                              |
| PMRF        | Perimeter moment resisting frames            |
| IGF         | Interior gravity frames                      |
| PP          | Perfectly pinned                             |
| SR          | Semi-rigid                                   |
| $R_\mu$     | Ductility reduction factor                   |
| $R_Q$       | Overstrength factor                          |
| $R_{\mu S}$ | Story ductility reduction factor             |
| $Q_{SL}$    | Ratio of story ductility to local ductility  |
| $Q_{GL}$    | Ratio of global ductility to local ductility |
| ESLM        | Equivalent static lateral method             |
| $\mu$       | Ductility                                    |